RESTORATION OF SANRIKU RAILWAY BY UTILIZING REINFORCED SOIL STRUCTURES TO ENHANCE EARTHQUAKE-AND-TSUNAMI-RESISTANCE

Yoshinori SHINDO[1] and Fumio TATSUOKA[2]

[1]Member of JSCE, Japan Railway Construction, Transport and Technology Agency (JRTT),
1st Design and Technology Division (6-50-1 Honcho, Naka-Ku, Yokohama-City, Kanagawa 231-8315, Japan)
E-mail: yos.shindo@jrtt.go.jp
[2]Members of JSCE, Professor, Dept. of Science and Technology, Tokyo University of Science
(2641 Yamazaki, Noda-Shi, Chiba 278-8510, Japan)
E-mail: tatsuoka@rs.noda.tus.ac.jp

A number of infrastructures for Sanriku Railway were seriously damaged by the 2011 East Japan Earthquake. In this paper, the damage by seismic loads and tsunamis are analyzed. In addition to serious damage by seismic loading, embankments, RC viaducts and bridges were washed away by the great tsunami in many places. A number of bridges and embankments could be effectively made highly earthquake- and tsunami-resistant by taking advantage of soil-reinforcing technologies. The design and construction in this restoration work took advantage of technologies that had been developed based on state-of-the-art geotechnical engineering, concrete engineering, and bridge engineering while aiming at cost-effective and fast restoration.

At Arakawa Bridge, the PCI girder was washed away and a new PC hollow girder with a small height, pier and geosynthetic-reinforced soil (GRS) embankment was installed. In the Shimanokoshi area, as requested by local people, a collapsed RC viaduct was replaced to a seismic- and tsunami-resistant geosynthetic-reinforced embankment covering slopes with concrete facing connected to geogrid layers reinforcing the embankment to prevent erosion of the backfill and scouring at the slope toes. At three places, in place of the collapsed three simple girder bridges, three GRS integral bridges, which are highly earthquake- and tsunami-resistant due to structural integration of reinforced backfill, full high rigid (FHR) facings and a continuous girder, were constructed and opened to service for the first time. In the existing embankments eroded by tsunami, the roadbed was restored by "reinforced roadbed" and embankment slope was covered with cast-in-place concrete facing or RRS (Reinforced Railroad/Road sloped structures with geocells and reinforcing steel bars) method.

Key Words : railway structure, geosynthetic-reinforced soil (GRS) embankment, GRS integral bridge, tsunami resistance

1. INTRODUCTION

The Sanriku Railway running along the Pacific Ocean coast side at Iwate Prefecture has two separate rail lines: South-Riasu Line from Sakari to Kamaishi and North-Riasu Line from Miyako to Kuji (**Fig. 1**). The railway facilities were damaged extensively by the 2011 Great East Japan Earthquake that occurred on March 11, 2011. **Table 1** summarizes the damage to the bridges and viaducts. Along the South-Riasu Line, a number of bridges were damaged by the

earthquake motion, while embankments were washed away by the tsunami in many places. Along the North-Riasu Line, a number of bridges, viaducts, and embankments were washed away by the tsunami[1]. Soon after the disaster, Sanriku Railway Company proposed a plan for the reconstruction of damaged infrastructures so that the whole line can be reopened on 6th April 2014. However the reconstructing term was very short, plus there was a lack of construction materials, equipment, and labor. Therefore it was a most important challenge to

Table 1 Outline of the damage to the bridges and viaducts.

Line	Sign	Bridge Name	Type of girder	Girder Span	Factor	Main damage
South Riasu Line	S-1	Sakarigawa Bridge	PCI girder	9@22.1m	motions	Pier, Bearing, Slab
	S-2	Arakawa Bridge	RCT girder, PC through-girder, PCI girder	19.8m+16.6m+32.1m	tsunami	Girder, Rail track
	S-3	1st Owatarigawa Bridge	PCI girder, Metal through truss girder	3@42.8m+71.6m	motions	Pier, Bearing, Slab
	S-4	Nakabanko Viaduct	RCT girder	10@22.9m	motions	Pier, Bearing, Slab
	S-5	2nd Owatarigawa Bridge	PCI girder, Metal through truss girder	3@35.8m+74.0m +2@50.0m+60.0m	motions	Pier, Bearing, Slab
North Riasu Line	N-1	Magisawa Bridge	2-span continuous PC through truss girder	2@36.0m	tsunami	Bearing, Rail track
	N-2	Shimanokoshi Viaduct	RCT girder, Rigid viaduct	14.5m+2@19.5m+15.2 m+19.5m+27.5m+8.4m	tsunami	Viaduct, Station, Rail track
	N-3	Matsumaegawa Bridge	PCI girder, RCT girder	35.9m+19.8m	tsunami	Girder, Pier, Rail track
	N-4	Koikorobe-sawa Bridge	RCT girder, PC hollow girder	19.8m+20.0m	tsunami	Girder, Embankment, Rail track
	N-5	Haipe-sawa Bridge	PC through-girder, RCT girder	32.1m+16.6m	tsunami	Girder, Embankment, Rail track

Note, PCI girder : Prestressed concrete girder with I-shaped main girders

RCT girder : Reinforced concrete girder with T-shaped section
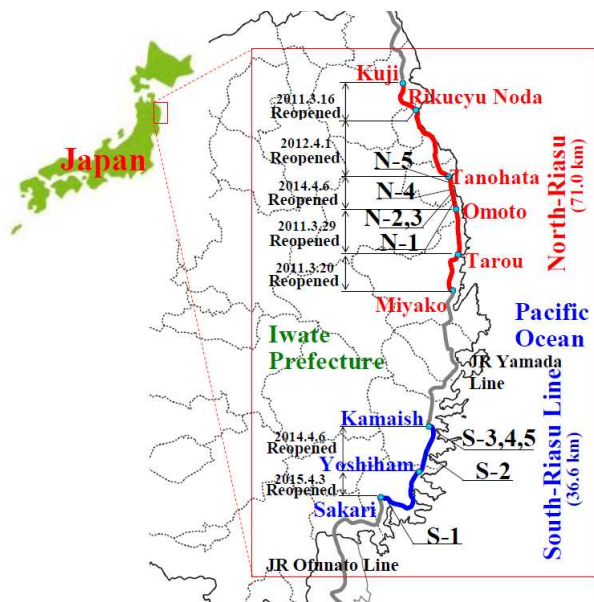
Fig. 1 Outline of Sanriku Railway.

shorten the construction term by applying a labor-saving efficient construction method and selecting a cost-effective structure type.

This paper reports the analyses of the disaster, the structure planning and design enhancing the resistance to earthquake and tsunami and the reconstruction in this project, which aimed to resume operation in the whole line of Sanriku Railway by April 2014.

2. DAMAGE BY THE TSUNAMI

The previous Arakawa Bridge of the South-Riasu Line was a three-span simple girder bridge consisting of a RCT girder, a PC through-girder and a PCI girder, located about 620 m upstream from the coast. The great tsunami running-up the river washed the PCI girder away (**Photo 1(a)**) [2]. The tsunami height was 14.07 m from the sea level [3, 4]. The PCI girder slab level was 14.15 m. It was likely that the lateral load and uplift applied to the PCI girder by the tsunami were very large due to the fact that the PCI girder height was 2.8 m and the bottom level was about 3.0 m lower than that of the PC through-girder.

Before the disaster, the railway structure in Shimanokoshi district of North-Riasu Line consisted of viaducts, a station and a two-span simple girder bridge, the Matsumaegawa Bridge. The great tsunami destroyed the viaducts and washed away the bridge (**Photo 1(b)** and **1(c)**). Koikorobe-sawa and Haipe-sawa Bridges were both two-span simple girder bridge. The tsunami washed away the girders, seriously damaged the abutments and eroded the approach embankments of these bridges (**Photo 1(d)** and **1(e)**). The through-girder of Haipe-sawa Bridge flowed for a distance of more than 50 m by the tsunami current and its web and slab exhibited a number of diagonal cracks (**Photo 1(f)**). It was likely that a large twisting load was exerted on the girder during the flow.

The railroad bed on the embankment was eroded and scored at many places (**Photo 1(g)**). Although the embankments had been constructed using gravel and rock from nearby tunnel excavation, the slope was also seriously eroded and scoured (**Photo 1(h)**).

3. RESTORATION OF ARAKAWA BRIDGE

To restore the damaged Arakawa Bridge, P2 pier and A2 abutment were reconstructed and a new 1.6

(a) Arakawa Bridge

(b) Shimanokoshi Viaduct

(c) Matsumaegawa Bridge

(d) Koikorobe-sawa Bridge

(e) Haipe-sawa Bridge

(f) diagonal crack

(g) Scoured and eroded roadbed

(h) Scored and eroded slope

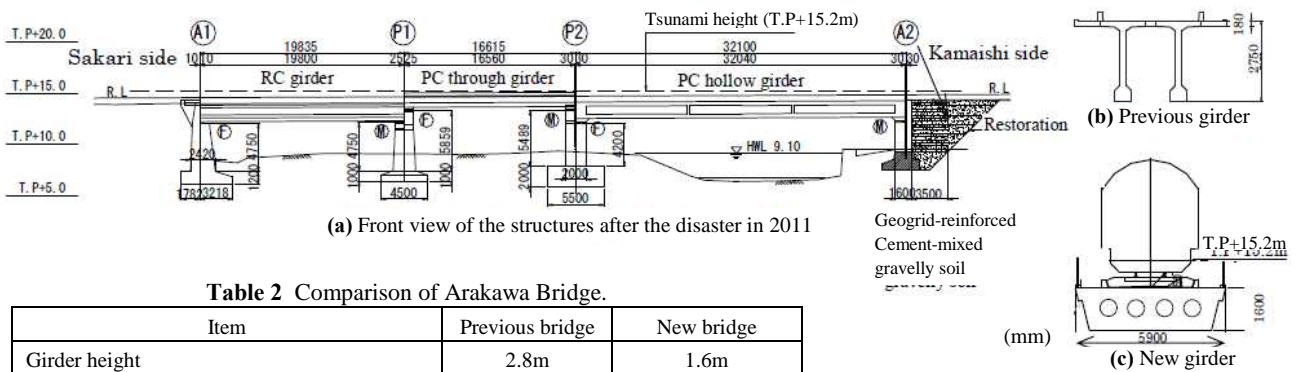**Photo 2** New Arakawa Bridge.

Photo 1 Damage by the tsunami.

(a) Front view of the structures after the disaster in 2011

(b) Previous girder

(c) New girder

Fig. 2 Arakawa Bridge.

Table 2 Comparison of Arakawa Bridge.

Item	Previous bridge	New bridge
Girder height	2.8m	1.6m
Lateral resistance / Lateral load by tsunami ※	0.22	0.71

※Refer to **Fig. 7**

m-height PC hollow girder was installed (**Photo 2** and **Fig. 2**). A PC hollow girder with a shorter height was selected to reduce the lateral tsunami load about 50% compared to the previous 2.8 m-high PCI girder. The new A2 abutment is a Geosynthetic-Reinforced Soil (GRS) structure that was designed to have sufficiently high resistance against the horizontal inertial load of the PC hollow girder exerted by design earthquakes.

(1) Structure of GRS abutment

The backfill of the approach block of GRS abutment is well-compacted cement-mixed gravelly soil that is reinforced with geogrid layers integrated to the back of the full high rigid (FHR) facing. In the conventional-type bridge abutment, a gravity-type abutment structure is constructed before the construction of the approach embankment. On the other hand, with the GRS abutment, the approach block is first constructed. **Fig. 3** shows in detail the con-

(a) Removal of damaged P2   **(b)** Newly constructed PC hollow girder   **(c)** Construction of A2 abutment

Photo 3 Restoration of Arakawa Bridge.

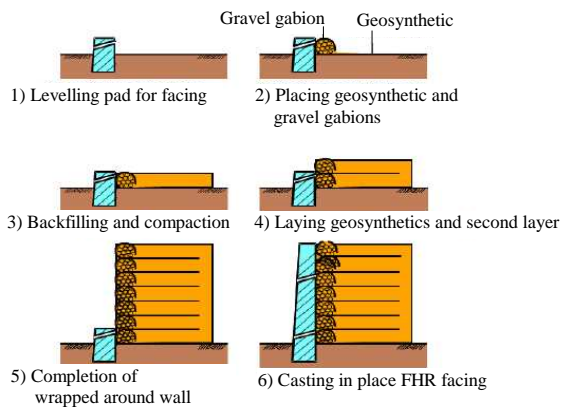**(a)** Matsumaegawa Bridge   **(b)** Koikorobe-sawa Bridge   **(c)** Haipe-sawa Bridge

Photo 4 Three completed GRS integral bridges for Sanriku railways.

Fig. 3 Construction procedure of GRS retaining wall.

struction procedure. Light cement-mixed backfill is compacted with the help of geogrid bags or wire mesh boxes filled with crushed stone placed at the edge of each 300 mm-thick soil layer arranged as a temporary facing structure. By repeating this step, a full-height wall is constructed. After the deformation of the supporting ground and approach block itself has sufficiently taken place, the FHR facing is constructed by casting in place fresh concrete in the space between the outer concrete form anchored in the backfill and the wall face wrapped around with geogrid reinforcement. As the fresh concrete passes through the mesh of the geogrid bags or wire mesh boxes and penetrates into the contained gravel of crushed stone, the facing is eventually firmly integrated to the cement-mixed backfill of the approach block.

As shown in **Fig. 2(a)**, the cement-mixed backfill was reinforced basically with 3.5 m-long short geogrid layers having allowable tensile rupture strength T_a of 30 kN/m at a vertical spacing of 300 mm. At every three layers of short geogrid, a long geogrid layer with T_a= 60 kN/m was arranged to the rear end of the approach block.

(2) Construction procedure of the girder

The original PC through-girder of the Arakawa Bridge was damaged only to a limited extent, and it was reused for the restoration. First, the PC through-girder was temporarily supported with a vent (**Photo 3(a)**). After the foundation and column of the new P2 pier was reconstructed, the PC through-girder was re-set using jacks. Then, fresh concrete was cast in place to construct the PC hollow girder (**Photo 3(b)**). Since the tensioning of the PC cables was a single pull-out only from the A2 abutment, the part of the approach block above the bearings on A2 was constructed after the tensioning of the PC cables. Then, the remaining part of the A2 abutment was constructed (**Photo 3(c)**).

4. RESTORATION OF THREE BRIDGES BY CONSTRUCTION OF GRS INTE-GRAL BRIDGES

The three bridges that collapsed by the tsunami, Matsumaegawa Bridge, Koikorobe-sawa Bridge, and Haipe-sawa Bridge, were reconstructed as GRS integral bridges (**Photos 4(a)-4(c)**). The new Matsu-

maegawa Bridge was constructed inside the new GRS embankment with the girder underlying 3.0m thick embankment (**Fig. 4** and **Photo 4(a)**). As Koikorobe-sawa Bridge passes over a local road, the previous simple girder bridge consisted of a PC girder and a RCT girder (see **Fig. 8**).

The PC girder had a large space between the girder and the ground surface. The newly constructed bridge has a continuous RC girder. Compared with the previous girder, the height of the new girder became lower, as the maximum moment at the center of the girder of a GRS integral bridge becomes very low (about a half at the maximum) due to the flexural moment at both ends of the girder that are integrated to the FHR facings. The Haipe-sawa Bridge also passes over a local road. Thus, the previous simple girder bridge also consisted of a PC through-girder and a RCT girder. The newly constructed GRS in-

tegral bridge has a continuous SRC through-girder. This is because, in the case of PC girder, contraction of the girder by pre-stressing should be restricted by the facing and the approach block. In the case of PC girders, elastic contraction by the pre-stress and long-term creep contraction take place in addition to the temperature contraction and dry shrinkage in the case of RC girders and SRC girders. This factor is important with relatively long girder.

(1) Characteristic features of GRS integral bridge
a) History of technology development [5), 6), 7)]
The GRS integral bridge is a new type bridge that was developed mainly by the second author and his colleagues and the researchers of Railway Technical Research Institute (RTRI). The first prototype was completed in 2012 as an over-road bridge at Kikonai for a new high-speed train line, Hokkaido Shinkansen.

A typical conventional abutment supports a simple girder via a pair of bearings (a roller and a hinge) placed on a pair of abutments that retain unreinforced backfill. The problems due to these structural characteristics include: 1) a high cost for the installation and long-term maintenance of the bearings; 2) development of harmful bumps immediately at the back of the abutment structures due to the settlement of the backfill, gradually for a long service time and suddenly by earthquakes; 3) massive abutment
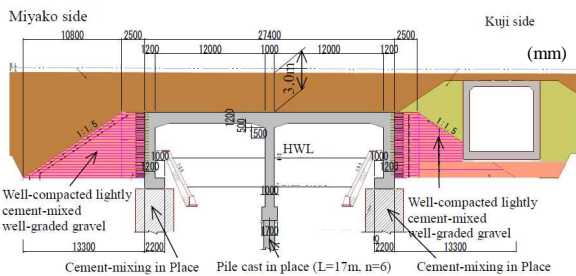

Fig. 4 Matsumaegawa Bridge (GRS integral bridge) at Shimanokoshi.
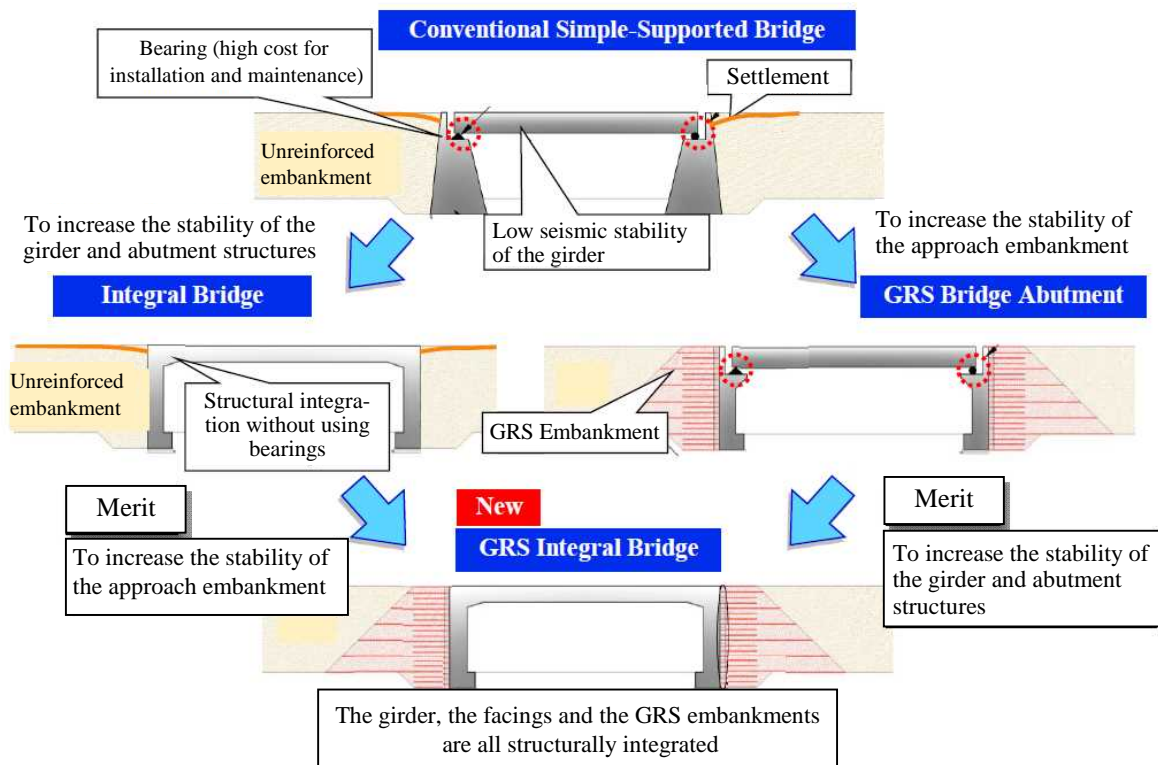

Fig. 5 History of technology development of GRS integral bridge.

structures often supported by pile foundations; and 4) a low seismic stability of the girder particularly at a bearing. To alleviate these problems, a new type of bridge structure, called GRS integral bridge, was developed by combining the technologies of integral bridge and GRS abutment (**Fig. 5**).

For a GRS integral bridge, the approach embankment is first constructed at both ends, If necessary for a long girder span, an intermediate pier (or piers) that support a continuous girder only vertically are also constructed. The zones of the approach embankments (called the approach blocks) are reinforced with geogrid layers connected to the FHR facings. To ensure high stability, the backfill of the approach block is lightly cement-mixed. After seven days, when the deformation of the supporting ground and the approach blocks has taken place, a pair of FHR facing is constructed by casting in place concrete so that the geogrid layers reinforcing the approach blocks are firmly connected to the FHR facings. Lastly, a continuous girder is constructed with both ends being integrated to the top of the facings not using bearings in the same way as the conventional integral bridge.

The advantages of structural integration among the girder, a pair of facing and a pair of approach blocks with GRS integral bridge are as follows:
1) The bridge is very stable without a possibility of dislodging at a bearing even during severe earthquakes.
2) Bumps by long-term and seismic loads do not develop immediately at the back of the facings.
3) Although active earth pressure or even higher earth pressure may be activated in the facings, as the facing is supported by geogrid layers at a short span (i.e., 300 mm) the facing becomes simple without pile foundation.
4) As the bending moment activated in the girder is reduced, the structure of the girder becomes simpler.

As a whole, GRS integral bridge is much more cost-effective while exhibiting a much higher stability, particularly against seismic loads and tsunamis, requiring a much less long-term maintenance cost.

b) Effects of thermal deformation of the girder on the performance of the abutments

With GRS integral bridge, due to the structural integration described above, the annual thermal expansion and contraction of the girder generate cyclic lateral compressional and tensile loads transmitted to the facing and then to the approach blocks. As the approach blocks are lightly cement-mixed gravelly soil, this thermal deformation is absorbed by a vertical thin buffer layer of uncemented gravelly soil
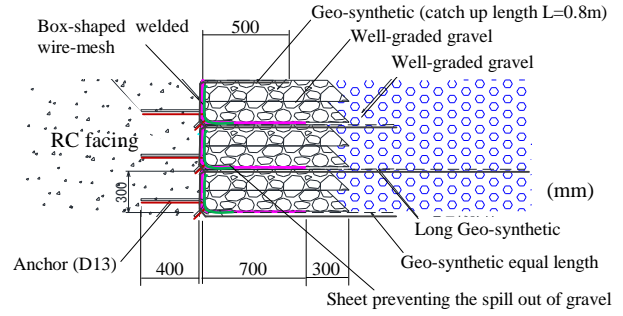
Fig. 6 Details of the connection part between the FHR facing and the GRS embankment.

placed between the facing and the approach block. To absorb relatively large thermal deformation of the relatively long girder, 40 m with Koikorobe-sawa Bridge and 60 m with Haipe-sawa Bridge, as shown in **Fig. 6**, the above mentioned buffer layer was made relatively wide, 1000 mm, composed of 700 mm-wide boxes of welded wire mesh containing unbound poorly graded gravel and 300 mm-wide zones of the same gravel type[8), 9)]. Welded wire mesh boxes were used for a larger width and also for labor saving in place of 400 mm-wide geogrid bags usually used for GRS retaining walls (**Fig. 3**).

(2) Tsunami resistance of GRS integral bridge
a) Tsunami loads activated on the girder

The tsunami loads activated on the girder shown in **Fig. 7** are calculated by the following equations proposed by Kosa[10)]:

$$Q_x = \rho g L \int_{z_1}^{z_2} (3.10\, a_H - z/0.42)\, dz, \quad Z/a_H \geqq 0.5 \quad (1a)$$

$$Q_x = 1.90 \rho g\, L, \quad Z/a_H < 0.5 \quad (1b)$$

$$Q_z = \rho g\, (0.53\, a_H - z/2.18) BL \quad (2)$$

where
Q_x : lateral load by tsunami
Q_z : uplift load by tsunami
a_H : the tsunami height
T : girder height
L : girder length $\quad B$: girder width
Z : center level of girder
z_1 : bottom level of girder ($= z$)
z_2 : formation level of girder
ρ : density of water
g : acceleration of gravity

b) Tsunami resistance mechanism

Figure 7 shows the mechanism of the resistance of GRS integral bridge against tsunami load[11)]. The lateral and lifting load that deep tsunami current applies to the girder is transmitted to the full high rigid (FHR) facing. The resistance by the submerged weight of the girder and facing is utterly insufficient to resist the loads by such deep tsunami current as the one by which the previous bridges totally collapsed.
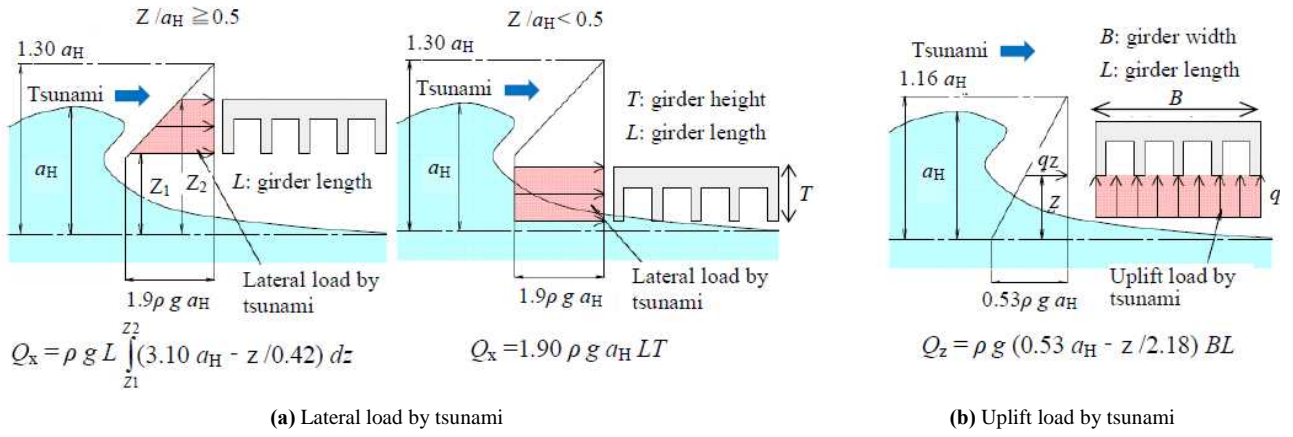
$$Q_x = \rho g L \int_{Z_1}^{Z_2} (3.10 \, a_H - z / 0.42) \, dz$$

$$Q_x = 1.90 \, \rho \, g \, a_H \, LT$$

$$Q_z = \rho \, g \, (0.53 \, a_H - z / 2.18) \, BL$$

(a) Lateral load by tsunami

(b) Uplift load by tsunami

Fig. 7 Schematic diagram showing the tsunami loads.
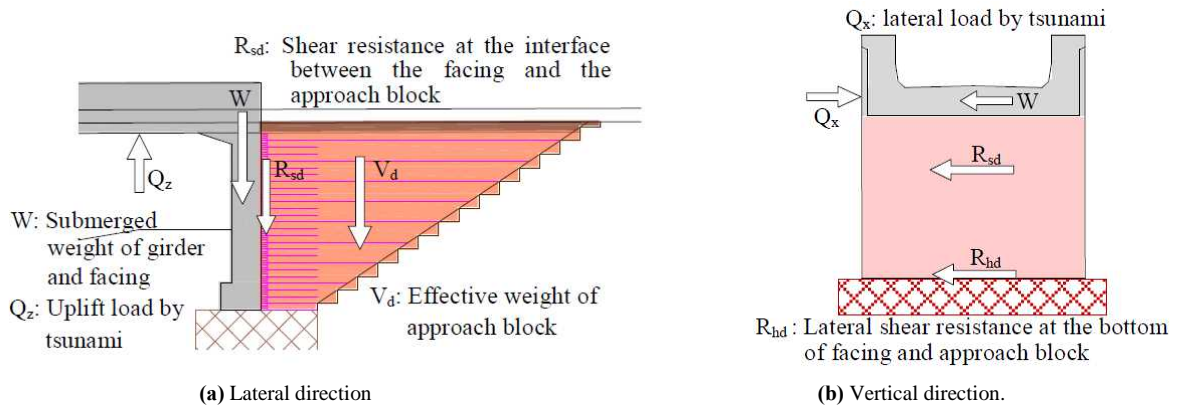

(a) Lateral direction

(b) Vertical direction.

Fig. 8 Resistance components against tsunami.

The tsunami loads exerted on the girder and facing are transmitted to the approach block via the buffer layer. The buffer layer exhibits the frictional shear strength of gravel developed by the confining pressure created by the tensile strength of the geogrid layers connected to the facing. Thus, the total submerged weight of the girder, facings and approach blocks resists the uplift of tsunamic current. The lateral shear strength at the bottom of the facing and approach blocks resists the lateral load of tsunami current.

The shear resistance at the interface between the FHR facing and the buffer layer was estimated as:

$$R_{sd} = B \, (n_1 \alpha_3 T_{1d} + n_2 \alpha_3 T_{2d}) \tan \delta \quad (3)$$

where

B : width of the FHR facing in the transversal direction of the bridge

n_1 : number of the equal length geogrid layers

n_2 : number of long geogrid layers

α_3 : correction coefficient in consideration of the rewinding of geogrid at the buffer layer (= 2)

T_{1d} : allowable tensile rupture strength (= 30kN/m)

T_{2d} : allowable tensile rupture strength (= 60kN/m)

δ : angle of shear resistance at the interface between the buffer layer and the FHR facing, assumed to

be equal to the internal angle of friction $\varphi = 40$ degrees of the gravel.

The vertical resistance at the bottom of the approach block against the tsunami uplift load was assumed to be equal to the sum of the submerged weight of the approach block (calculated using the total saturated weight γ equal to 20.0 kN/m^3 of well-graded gravelly soil) and the girder weight with facings.

The lateral resistance at the bottom of the approach block was set equal to:

$$R_{hd} = f_{rb} \, (V_d \tan \delta_b + A' \, c') \quad (4)$$

where

V_d : effective weight of approach block

f_{rb} : ground resistance coefficient with respect to the lateral support force (= 1.0)

δ_b : angle of shear resistance δ_b (set equal to the angle of internal friction $\varphi = 35$ degrees of the supporting ground)

$A'c'$: adhesion at the interface between the footing bottom and the supporting ground, which was set equal to zero assuming that the supporting ground below the facing bottom was scoured by the tsunami.

16

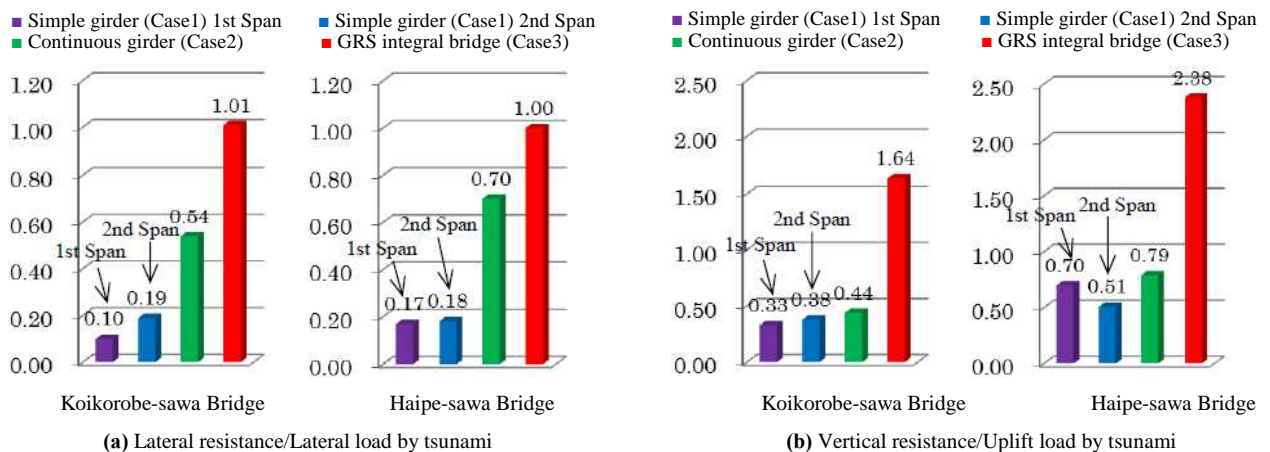## c) Analysis of stability against tsunami

Figure 9 compares the stabilities against the tsunami load described in **Fig. 7** of the three bridge types at Koikorobe-sawa and Haipe-sawa. In **Fig.7**, w is the weight of the girder. Case 1 is the simple girder bridge-type that was washed away by the tsunami. Case 2 is a continuous girder bridge of which both ends are supported at the top of the RC abutment structures with bearings. Case 3 is GRS integral bridge that was actually constructed to restore the bridges. The tsunami height measured near Koikorobe-sawa Bridge was 21 m, compared with a rail level equal to 12.3 m from the sea level and the one measured near the Haipe-sawa Bridge was 19.0 m, compared with a rail level equal to 14.4 m. The following calculation conditions were adopted: i.e., for Koikorobe-sawa Bridge, a_H is 21.0 m and z_2 is 12.3 m; and, for Haipe-sawa Bridge, a_H is 19.0 m and z_2 is 14.4 m. The resistance of the respective bridge types was calculated as follows:

1) Simple girder bridge: The lateral resistance of a simple girder is equal to the lateral resistance coefficient $\mu = 0.6$ times the submerged girder weight (equal to the total weight minus the buoyancy). Here, μ is the seismic design coefficient of restrainers (steel plain bar stopper). The vertical re-
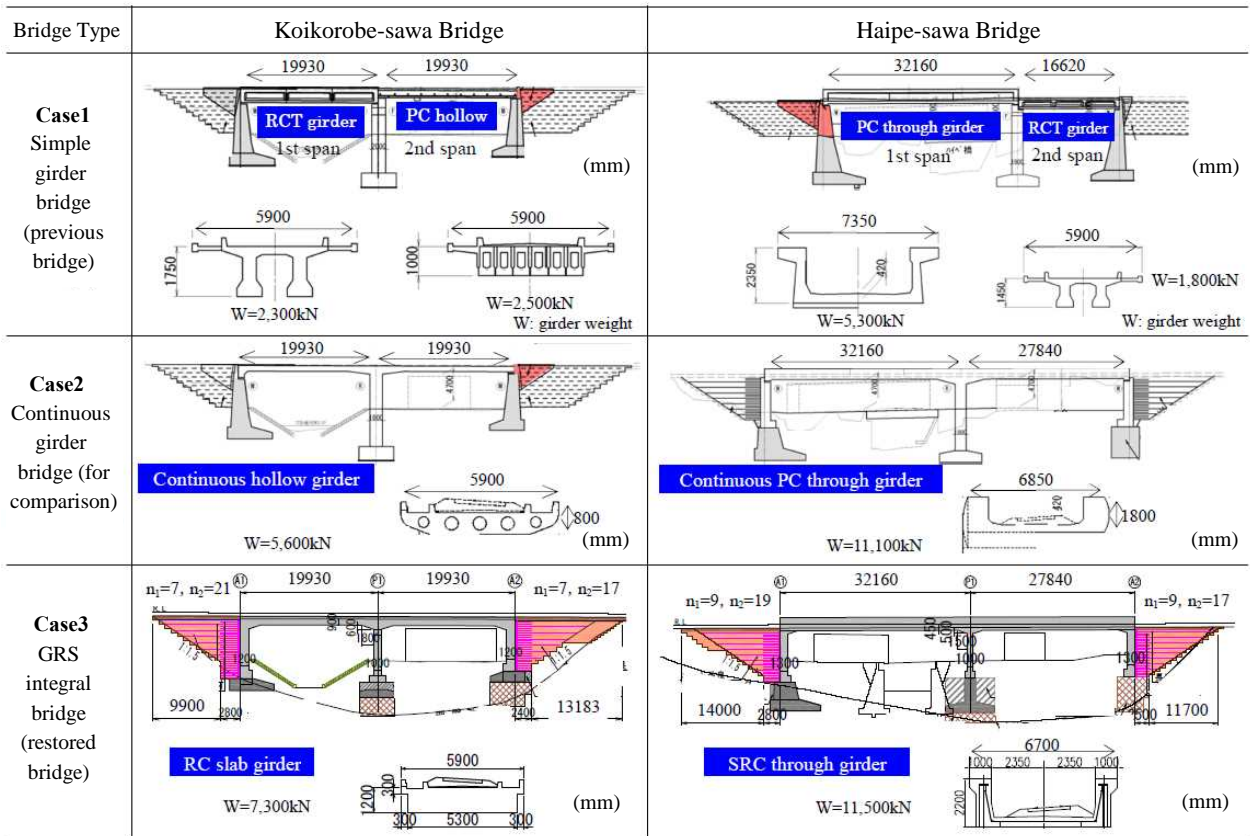
Fig. 9 Different bridge types compared at the design of Koikorobe-sawa Bridge and Haipe-sawa Bridge.

(a) Lateral resistance/Lateral load by tsunami   **(b)** Vertical resistance/Uplift load by tsunami

Fig. 10 Analysis of the stability against tsunami of different bridge types at Koikorobe-sawa Bridge and Haipe-sawa Bridge.

sistance is equal to the submerged weight of the girder only.

2) Continuous girder bridge: The lateral resistance of a continuous girder is equal to the design value of lateral seismic coefficient for the stopper $\mu = 1.2$ times the submerged girder weight. The vertical resistance is equal to the submerged girder weight only.

3) GRS integral bridge: The lateral resistance of the whole bridge system is equal to the smaller of R_{sd} or R_{hd} plus the submerged girder weight. The vertical resistance is equal to the total submerged girder weight plus the smaller value of R_{sd} or V_d.
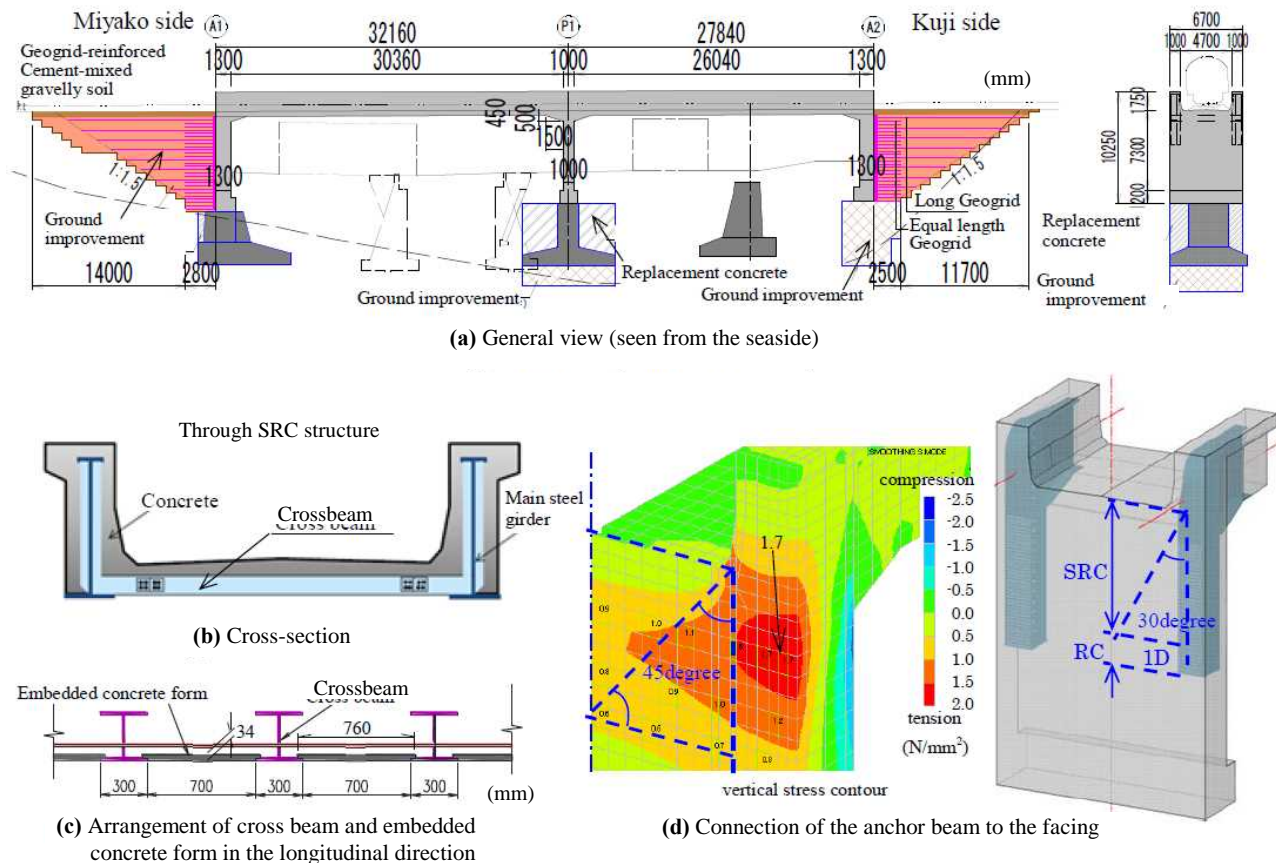
Figure 10(a) compares the ratios of the lateral resistance to the lateral tsunami load of the three bridge types at the two sites, while **Fig. 10(b)** compares the ratios of the vertical resistance to the tsunami uplift load. It may be seen that, with the simple girder bridge and the continuous girder bridge, the ratio is substantially lower than 1.0 showing a very low stability against the considered tsunami load. This is due to the fact that the tsunami load applied to the girder is resisted only by the girder weight, so the resistance is low. On the other hand, with the GRS integral bridge, the ratio is high, equal to, or higher than, unity, showing a particularly high stability. This feature can be attributed to the fact that the

weight of the facing and approach block is added to that of the girder in resisting against the tsunami load. Kawabe et al.[12] performed model tests in the laboratory and showed that a GRS integral bridge is much more stable than a simple girder bridge against deep tsunami current.

(3) Design of GRS integral bridge (Haipe-sawa Bridge) [13]

a) Span arrangement

The continuous girder of the GRS integral bridge at Haipe-sawa is vertically supported by a pier at its center. To have a sufficient free height between the ground surface and the girder accommodating an under-passing local road, a through-girder was adopted in the same way as the previous bridge. For the girder, a SRC structure was adopted for a good constructability, easier rigid connection to the top of the facing and a high long-term durability. The abutment shown on the right side in **Fig. 11(a)** had moved towards the right for a distance of 12 m from the location of the original abutment of the previous bridge. This is because the left side span (between the left side abutment and the central pier) and the right side span (between the pier and the right side abutment) should be balanced as a continuous bridge, while the left side span is required to be 32.16

(a) General view (seen from the seaside)

(b) Cross-section

(c) Arrangement of cross beam and embedded concrete form in the longitudinal direction

(d) Connection of the anchor beam to the facing

Fig. 11 Structure overview of Haipe-sawa Bridge.

(a) GRS abutment   **(b)** Erection of steel main girder   **(c)** Mechanical joint

Photo 5 Construction of Haipe-sawa GRS integral bridge.

m-long to accommodate the local road. Then, the right side span became 27.84 m-long and the total span became 60 m, which is the longest so far for a GRS integral bridge. The area of the opening below the right side span increased to 290 m^2 from the previous 200 m^2, which would reduce the dam-up height of tsunami.

b) Design of foundation

The seismic inertia of the girder and facing is mainly supported by both approach blocks. Therefore, the sub-grade reaction at the foundations of the facing and the pier is smaller than that of the conventional simple girder bridge. To shorten the construction period and to reduce the amount of construction waste, as shown in **Fig. 11(a)**, the sound part of the foundations of the previous bridge that survived the tsunami was re-used for the foundations of the GRS integral bridge.

c) Design of girder

The SRC through structure is composed of a pair of main steel girders, a number of steel crossbeams, and a pair of anchor beams at both ends (**Figs. 11(b)** and **11(c)**). When the bottom face of the lower flanges of the steel I beams of the main steel girders and the steel crossbeams is covered with a concrete layer, the total slab thickness becomes greater than 600 mm, which is not allowable to ensure the free height under the girder. In addition, the provision of the space for concrete placing work becomes necessary under the girder, which does not allow large vehicles to pass through under the girder during the construction. Thus, it was decided to expose the bottom face of the lower flanges of the main steel girders and the steel crossbeams and to cover the other areas at the bottom of the girder with embedded concrete forms (each 760 mm × 940 mm & t= 34 mm) (**Fig. 11(c)**). Both ends of the respective forms were arranged on the lower flanges of the crossbeams. As a result, the space below the girder became free during the construction. Besides, the slab became 450 mm-thick, while the free height under the girder became more than 4.7 m with an allowance

of 100 mm. To shorten the construction period, to save labor work and to improve the long-term durability, the concrete layer outside the main girder was also placed in embedded forms that formed the lateral outer face of the SRC girder.

d) Connection of joint girder to FHR facing

The girder was structurally integrated to the top of the FHR facing by arranging a steel anchor beam at the respective ends of the steel main girder (**Fig. 11(d)**). The length of the vertical flange of the anchor beam was determined based on the stress distribution caused by train roads of the girder evaluated by FEM analysis. According to the analysis, high stresses distribute in a fan-shaped zone with an apex angle of 45 degrees as shown in **Fig. 11(d)**. For safety, the high-stress zone was assumed to be a fan-shaped zone with an apex angle of 30 degrees, resulting in a longer flange, which was supported by a SRC structure covering the fan-shaped zone and an additional zone of RC structure with a height equal to the width D of the flange [14].

(4) Construction of GRS integral bridge at Haipe-sawa

Haipe-sawa Bridge was constructed as follows: a) preparation of the supporting ground for the GRS abutments; b) improvement of the supporting ground below the existing and new footings; c) placement of concrete covering the existing footing for the central pier; d) construction of the approach blocks of GRS abutments; e) construction of the FHR facing connected to the approach blocks; f) erection of the steel structure of the girder; and g) casting in place of the concrete for the girder with connection to the FHR facing.

a) Ground improvement

For a sufficient bearing capacity of the foundations for the bridge, the subsoil layer between the ground surface and the bedrock supporting the central pier (P1) and the right side abutment (A2) was improved by the high-pressure injection method. To this end, 12 holes were drilled in the existing footing

of pier P1 to insert a double-pipe rod that supplies cement slurry into the ground for the high-pressure injection method. Improved soil piles of a diameter of 3.6 m with a target uniaxial compressive strength equal to 3.0 MPa were formed in the subsoil layer. In order to confirm the strength of the improved soil, pressure meter tests were performed in the periphery of several improved soil piles, and it was confirmed that the uniaxial compressive strength was 5.8 MPa or higher.

Replacement concrete was cast above the existing footing of pier P1 to form a spread foundation of the new pier P1.

b) Construction of GRS abutment [15]

The approach blocks were constructed by compacting well-graded gravelly soil mixed with blast slag cement type B with 3 % weight of the gravel (**Photo 5(a)**). The amount of the cement was determined by performing unconfined compression tests in the laboratory. Each 300 mm-thick soil layer between the vertically adjacent geogrid layers consisted of two 150 mm-thick compacted soil layers. Based on the results of field compaction tests performed at the site, compaction method was that a 10 ton-class flat steel vibratory roller was passed six times on a 200 mm-thick spread soil layer to achieve a degree of compaction D_c equal to at least 92% with an average equal to, or higher than, 95%. D_c is the ratio of the field dry density ρ_d measured at nine points in every three soil layers by the RI (radioisotope) method to the maximum dry density $(\rho_d)_{max}$ determined by the laboratory compaction test following the "E-b" method (modified Proctor, 4.5Ec) according to JIS A1210. The quality of the compacted soil was evaluated also by measuring the coefficient of vertical subgrade reaction K_{30} by the FWD (Falling Weight Deflectometer) test on the compacted soil layer. It was confirmed that the measured K_{30} values satisfied the required values, at least 70 MN/m^3 with an average equal to or higher than, 110 MN/m^3.

c) Construction of the girder

The steel girder was constructed by assembling the members on the ground then erecting the girder using the crane vent method (**Photo 5(b)**). After the erection of the steel girder, the support was removed. At that stage, the steel girder was to support the casting load of concrete and it was necessary to prepare for possible aftershocks during the construction. Therefore, a pair of anchor beams at each end of the steel girder was stabilized by connecting to each other with a brace. In the FHR facing, a mechanical-type connection was used for main rebar joints, because the gas pressure joint could not be

used due to close proximity to geogrid layers arranged at the back of the facing (**Photo. 5(c)**). Concrete was cast first at the span part of the bridge, then at the connection part between the girder and the FHR facing. In the zones including the construction joint where concrete was cast, at the last stage, expanding concrete was cast to prevent the formation of cracks.

5. STRUCTURE CHANGE FROM THE VIADUCT TO GRS EMBANKMENT (SHIMANOKOSHI DISTRICT)

### (1) Overview of the embankment

The damaged railway at Shimanokoshi area was reconstructed in conjunction with the restoration plan of the local government. The viaduct was replaced with an embankment that also functions as a tsunami barrier (**Fig. 12**). The embankment is required to satisfy "performance rank II" according to the design standard for railway structures and commentary (Earth structures) [15]. The "performance rank II" requires the embankments not to reach devastating failure under the Level-2 earthquake motions [16] (i.e., very strong inland earthquakes that may take place rarely during the design life) and the deformation should not become larger than the one that can be dealt with by regular maintenance under ordinary conditions. The seismic design standard was revised in 2012, while the design of Shimanokoshi area started in 2011. Therefore the seismic design standard of 1999 was applied to this case.

The dimensions of the embankment are such that the crest width is 5.9 m; the average embankment height is 8.7 m; the slope gradient is 1:1.8; and the bottom width is about 40 m (**Fig. 13**). The slope surface is covered with cast in place concrete facing to prevent erosion by the tsunami. A box culvert was constructed at a location that crosses a local road. A GRS integral bridge with a central pier was constructed to accommodate Matsumae-River. The Shimanokoshi Station, which was previously located on the viaduct, was transferred onto the embankment at the Kuji side (**Figs. 12(b)** and **12(c)**). The local municipality constructed this new station office and the embankment for the station square.
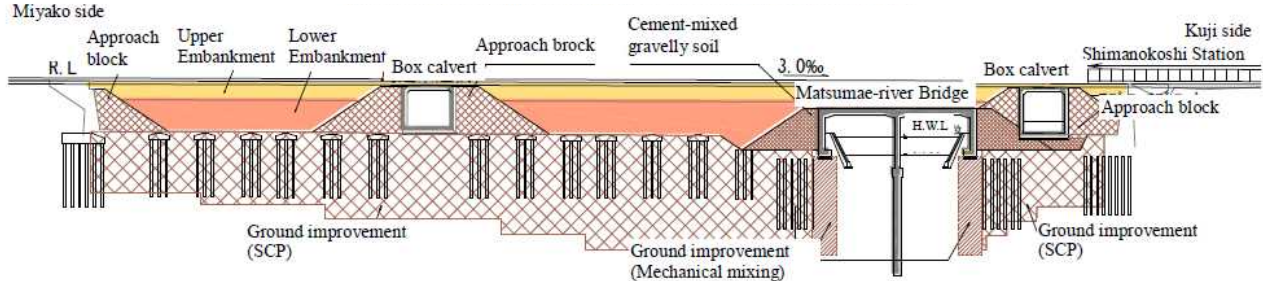
(2) Ground improvement
### a) Evaluation of liquefaction potential

The potential for soil liquefaction in the design of railway structures is evaluated by comparing the liquefaction strength ratio with the maximum share stress ratio as expressed by the following equation:
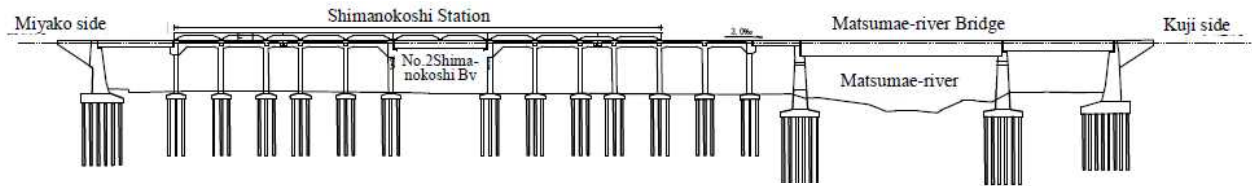
(a) Front view of the previous structures before the disaster in 2011

(b) Front view of the structures newly constructed after the disaster in 2011
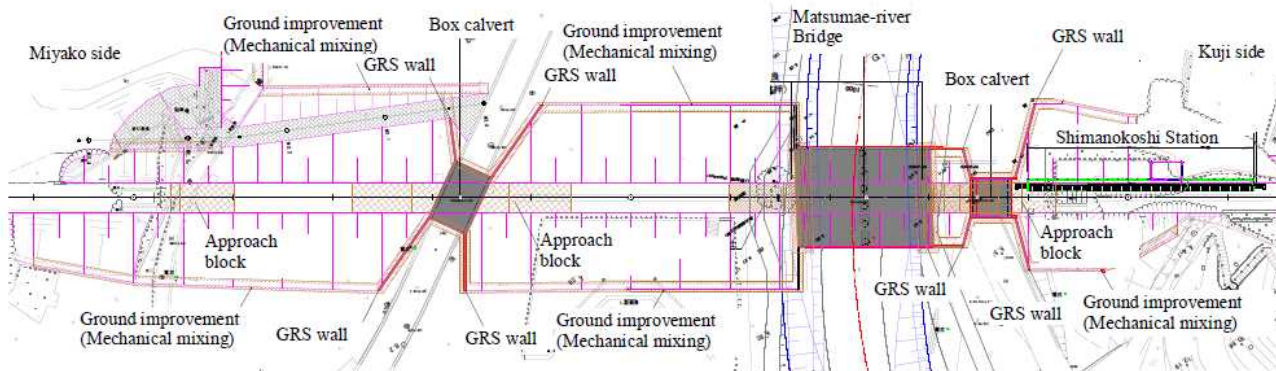
(c) Plan view of the structures newly constructed after the disaster in 2011

Fig. 12 Restoration of Shimanokoshi district.

$$F_L = R / L \qquad (5)$$

where

F_L : factor of liquefaction resistance

R : strength ratio causing liquefaction

L : maximum share stress ratio

The range of the ground that should be improved was determined based on the liquefaction potential index defined as:

$$P_L = (1 - F_L)\, w\, dz, \quad w = 10 - 0.5\, z \qquad (6)$$

where

P_L : liquefaction potential index

z : the depth in maters

Table 3 shows the relationship between the liquefaction potential index P_L and the evaluated degree of liquefaction of ground.

The embankment is underlain by a 15m to 25m-thick alluvium deposited on the bedrock. The upper layer is sandy soil with an average N value equal to 10 and the lower is gravelly soil. The classified ground type [16] is G2 ground with a natural period of surface ground T_g less than 0.25 s at the Miyako side (on the left side in **Fig. 12**) and G3 ground with T_g from 0.25 to 0.5s at the Kuji side. The
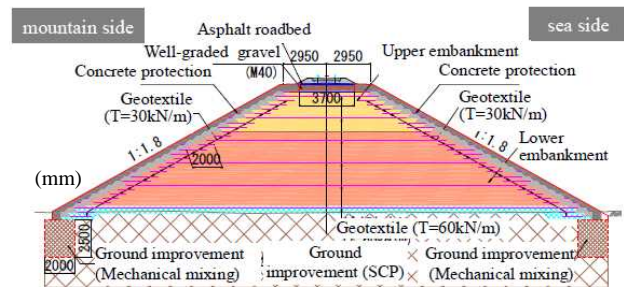

Fig. 13 Standard cross-section of GRS embankment.

Table 3 Relation between P_L and the degree of liquefaction.

P_L	degree of liquefaction for the ground	
	Risk of liquefaction	evaluation of liquefaction
$0 < P_L \leqq 5$	low	unnecessary
$5 < P_L \leqq 20$	high	necessary
$20 < P_L$	very high	necessary

liquefaction potential of the alluvium layer against Level-2 design earthquake motion spectrum type II

(a) Ground improvement

(b) Construction of measures to prevent scour by overflowing tsunami

(c) Constructing of embankment

Photo 6 Construction of measures to prevent scour by overflowing tsunami.

Table 4 Material and compaction control for performance rank II of the embankments.

Item	Approach block	Upper part of the embankment	Lower part of the embankment
Properties and classified soil types	· Well-graded gravel · Specific gravity : higher than 2.45 · Water absorption : below 3.0% · Abrasion weight loss : below 30%	· Group A, B ※ · Stabilized Group C, D1, V ※ ※Recycling resources does not apply	· Group A, B ※ · Stabilized Group C, D1,D2, V ※ · Use of recycled crushed concrete is allowed

Strength Compaction degree	· 1layer:300 mm
	  Each compacted soil layer:150mm-thick
	· Compaction density ratio D
	  Degree of compaction (4.5Ec)
	  Average $\geqq$ 95 %, Lower limit $\geqq$ 92 %
	· Well-graded gravel
	  $K_{30} \geqq$ 110 MN/m³
	· Cement-treated approach block
	  Uniaxial compressive strength :
	  $q_u \geqq$ 2000 kN/m²
		· Compaction density ratio D
		  Degree of compaction (4.5Ec)
		  Average$\geqq$90 %, Lower limit$\geqq$87 %
		· K_{30} Value
		  70MN/m³(Lower limit 50MN/m³)
		  $\leqq$ Average
		  $\leqq$110MN/m³(Lower limit 70MN/m³)
		  or
		  110MN/m³$\leqq$ Average,
		  Lower limit $\geqq$ 70MN/m³
			· Compaction density ratio D
			  Degree of compaction (4.5Ec)
			  Average$\geqq$90 %, Lower limit$\geqq$87 %

※ Group A, B, C, D1, D2 and V : Refer to Design Standards for Railway Structures and Commentary (Earth structures)

was evaluated. The evaluated liquefaction potential index P_L ranged from 19.0 to 42.8. When P_L is larger than 15, the soil layer is considered likely to liquefy requiring measures to prevent liquefaction [16]. There are several possible anti-liquefaction measures, such as vibrating rod compaction method, sand (gravel) compaction pile method (hereafter referred to as the "SCP"), mechanical mixing method, pile net method and so on. The SCP method (**Photo 6(a)**) was selected because of many previous successful cases and validated high effects, as well as a short construction period, which was required for the railway to be re-opened as scheduled (i.e., 6th April 2014).

b) Implementation of anti-liquefaction measures

It was found by a site investigation making several bore holes that a large amount of boulders and large gravel particles existed in the soil layer are required improvement. Therefore, a total number of 1,934 vertical holes with a diameter of 500mm were drilled by using an earth auger. Then, casing pipes with 400 mm in diameter were installed in the bored holes. Finally, crushed stones were thrown into the casing pipes and compacted to form improved gravel piles with a diameter of 700 mm. The length of the gravel piles ranged from 5 to 20m with an interval ranging

Table 5 Changes in the P_L value (L2,SP II).

Location	A	B	C	D	E	F
Before improvement	29.3	29.7	19.0	26.9	36.0	20.4
After improvement	0.50	3.30	0.40	3.93	2.12	3.89

from 1.2 m to 2.4 m. In this work, reused gravel with a volume of 7,700m³ obtained by recycled crushed concrete and gravel with a volume of 10,000m³ obtained by crushing hardrock stone from nearby tunnel excavation were used. The effects of this ground improvement work was confirmed by boring at the diagonal center of four gravel piles, close to the location of boring performed before the ground improvement work. It may be seen from **Table 5** that the P_L values decreased substantially as a result of this ground improvement work to values noticeably lower than 5, indicating a very low possibility of liquefaction (**Table 3**).

c) Measures to prevent scour at the slope toe

The overtopping tsunami current may scour the ground below and in front of the toe of the downstream slope (i.e., inland slope) of the embankment. To prevent such damage as described above with the

newly constructed embankment, as indicated in **Fig. 13**, this part of the ground was improved by mechanical cement-mixing in place (**Photo 6(b)**). The improved depth was 2.5 m and the width was 2.0 m. The design uniaxial compressive strength after a curing period of 28 days of the improved soil was 1,000 kN/m^2.

(3) Construction of embankment
a) Selection of fill material

For a total volume of the newly constructed embankment of 27,000 m^3, the fill material was generally in shortage due to many other restoration and construction projects in progress. Thus, the surplus soil with a volume of 10,100 m^3 generated by drilling in the SCP work and reused gravel of crushed concrete (12,500 m^3) were used as the fill material for the lower part of the embankment satisfying the design standard specified for railway soil structures. As the fill material for the upper part of the embankment, crushed gravel of hardrock stone from nearby tunnel excavation was used. Well-graded gravel was used as the fill material for the approach blocks.

b) Construction of embankment

On respective compacted soil layers in the embankment (**Fig. 13**), short geogrid layers with an allowable tensile rupture strength T_a equal to 30 kN/m were arranged in a vertical spacing of 0.3 m and long geogrid layers with T_a= 60 kN/m were arranged for a full width of the embankment in a vertical spacing of 1.5 m (**Photo 6(c)**). For a lift equal to 0.3 m, the compaction machine type and the number of passing were determined based on the results of trial compaction tests at the site. The specifications for the degree of compaction and K_{30} values in compaction control to satisfy "performance rank II" specified in the design standard for railway soil structures are listed in **Table 4**. The field soil dry density was measured by the RI (radioisotope) method and the number of passing of the compaction machine was monitored by using GPS.

6. RESTORATION OF EXISTING EMBANKMENTS

At many other places, tracks and roadbeds on the embankment along the sea shore of North-Riasu Line were washed away by the tsunami (**Photo 1(g)**) and/or the slope were eroded (**Photo 1(h)**). Yet, the main body of the embankment could survive the tsunami. Therefore, it was decided to restore these damaged embankments as follows, without full reconstruction. **Fig. 14** shows the partial restoration procedure of embankment. At step 1, cutting the slope that was scoured and eroded by tsunami and
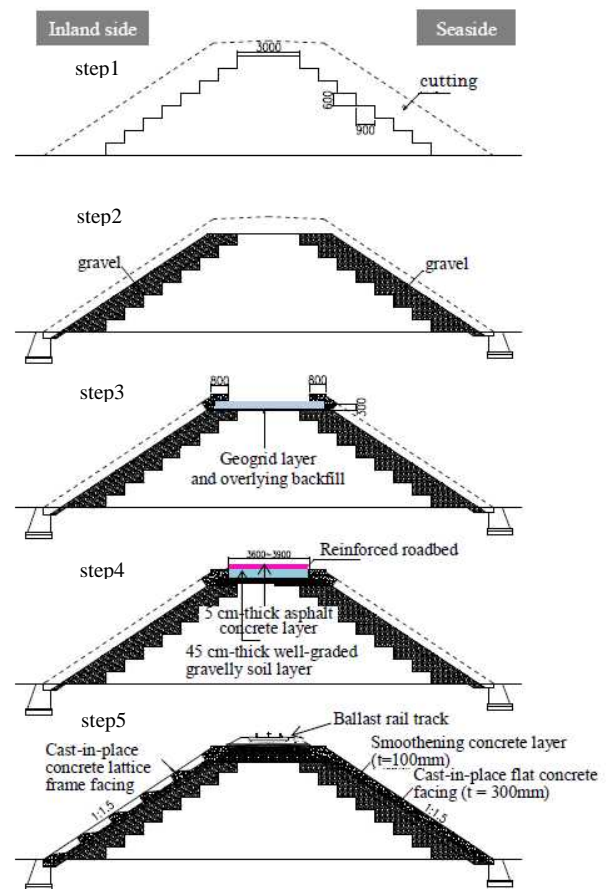

Fig. 14 Partial restoration procedure of embankment.

Photo 7 Side slopes of the embankment and the geogrid layer.

(a) Seaside slope covered with a cast in place concrete facing

(b) Inland side slope covered with a cast in place concrete lattice frame

Photo 8 Embankment after restoration.

replacing the slope by the well gravel at step 2.

(1) Restoration of roadbed

The roadbed on the embankment crest that was washed away was restored by constructing a ballast track on a 50 mm-thick asphalt concrete layer overlying a 450 mm-thick well-compacted well-graded gravelly soil layer (herein referred to as "the reinforced roadbed") to prevent wash-away of the roadbed (at step 4 in **Fig. 14**). In this case, "performance rank II" is required in respect to safety for the embankment according to the design standard for railway structures. Then, the K_{30} values measured by plate loading tests at the crest of the embankment are required to be at least 70 MN/m^3. When the K_{30} value is lower than 70 MN/m^3, as shown in **Fig. 14** at step 3, a geogrid layer is arranged at a depth of 300 mm from the bottom of the well-graded gravelly soil layer of the reinforced roadbed so that the reinforced roadbed can be well roller-compacted (as shown in **Photo 7**), prior to the construction of a concrete facing on the side slopes of the embankment. The geogrid layer was finally connected to the concrete facings on the crest and both slopes of the embankment at step 3 in **Fig. 14**.

(2) Restoration of embankment slope
a) Recovery with cast in place concrete

Conventionally, the slopes of coastal embankments, including those constructed as a tsunami barrier, are covered by pre-cast concrete panels just placed on the slope of unreinforced embankment. However, the slopes of the restored embankment were covered with continuous cast in place concrete facings reinforced with continuous steel reinforcement bars while connected to the geogrid layers reinforcing the embankment. In this way, the concrete facings become much more difficult to be peeled off by strong overtopping tsunami currents. The sea side slope was covered with a cast in place flat concrete facing (**Photo 8(a)**). The inland side slope was covered with a lattice frame made of cast in place concrete to more effectively protect the slope from erosion by reducing the energy of overtopping tsunami current (**Photo 8(b)**). The construction procedure is illustrated in **Fig. 14**. These concrete facings on the slopes were constructed (at step 5 in **Fig. 14**) after the deformation of the embankment and supporting ground has taken place so that the facings are not damaged by such deformation as above.

For a high durability of the horizontal seams between the concrete facing at the crest, which had been already constructed (at step 3 in **Fig. 14**), and those at the side slopes, the crack prevention rebars were arranged in the concrete layer on the slopes while the seams were coated with impregnated waterproofing agent.
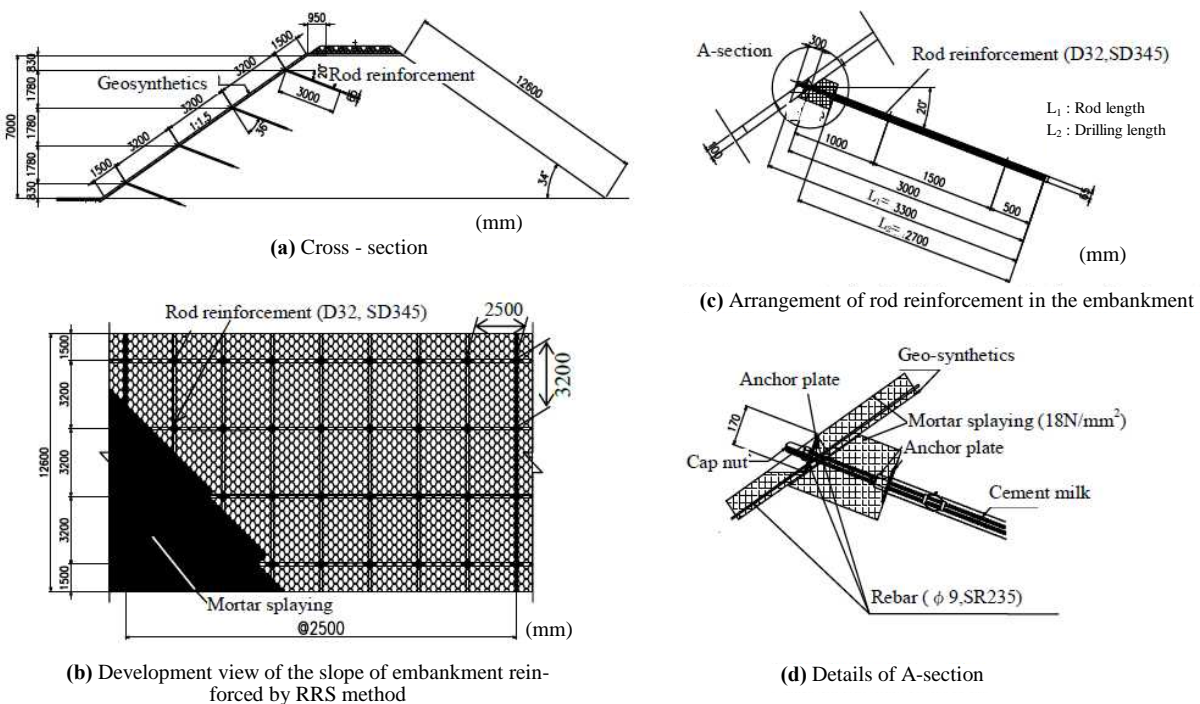

(a) Cross - section

(c) Arrangement of rod reinforcement in the embankment

(b) Development view of the slope of embankment reinforced by RRS method

(d) Details of A-section

Fig. 15 Reinforcement of existing embankment by RRS method.

(a) Insertion of the rod into the embankment   **(b)** Arrangement of geocell on the slope   **(c)** Shotcreting on geocell

Photo 9 Reinforcement of existing embankment by RRS method.

b) Restoration of damaged embankments by RRS method [17)]

The embankments of South-Riasu Line were also damaged by overtopping tsunami current at many places. To efficiently restore the damaged embankments and give them high resistance against overtopping tsunami current, the embankments with rock-covered slope, which were not necessary to be entirely reconstructed were reinforced by the RRS (Reinforced Railroad/road Sloped structures with geocells and reinforcing steel bars) method (**Fig. 15** and **Photo 9**). The RRS method made it possible to shorten the restoration term. The RRS method combines the slope stabilization technology by nailing and the slope surface protection technology using a geocell. This method was executed as follows: 1) Holes with a diameter of 65 mm were drilled into the embankment; 2) Metal rod reinforcement, D32 and SD345, with an effective length of 3.0 m were inserted into the drilled holes (**Photo 9(a)**); 3) Geocell with a cell height of 100 mm was arranged on the slope (**Photo 9(b)**); 4) Finally, the inside of the cells was filled with shotcrete (**Photo 9(c)**).

7. SUMMARY

The restoration work on the structures of Sanriku railway damaged by seismic loads and overtopping tsunami currents during the 2011 Great East Japan Earthquake reported in this paper can be summarized as follows:

1) The restoration term was shortened and made more cost-effective by applying several soil-reinforcing technologies, including geosynthetic-reinforced soil (GRS) for entirely reconstructed embankments and nailing for existing embankments that were partially reconstructed. Consequently, the railway was reopened as scheduled on 6th April 2014.

2) Four bridges of which the girder, the foundation and the approach embankments were washed away by the tsunami were restored by using the GRS technology. One bridge was restored by constructing a GRS bridge abutment and adopting a simple-supported PC hollow girder to enhance the tsunami resistance. Three bridges were restored by constructing GRS integral bridges. With this new bridge type, a continuous girder is structurally integrated to the top of a pair of facings (i.e., RC abutment structures) that are integrated to approach embankments that are reinforced with geogrid layers connected to the facings. Compared with the previous conventional simple girder bridges that fully collapsed as a result of the earthquake, GRS integral bridges have much higher resistance against seismic and tsunami loads while requiring much less maintenance cost.

3) The previous viaduct that fully collapsed due to the tsunami was reconstructed to the GRS embankment to function also as a tsunami barrier meeting the disaster prevention plan of the local municipality.

4) Less damaged embankments were restored by taking advantage of the technologies of nailing and slope protection using a geocell without entire reconstruction.

REFERENCES
1) Noda, G. and Shindo, Y. : Damage situation of the recovery plan Sanriku Railway, *The Foundation Engineering and Equipment*, Vol. 40, pp. 62-64, 2014 (in Japanese).
2) Shindo, Y., Sasaki, K., Koda, F. and Noda, G. : Restoration of Sanriku railway bridges that were damaged by the Great East Japan Earthquake, *Journal of Prestressed Concrete*, Vol. 57, pp. 62-67 , 2015 (in Japanese).
3) Preliminary estimates by the Tohoku-Pacific Ocean earthquake tsunami joint investigation group : http://www.coastal.jp/ttjt/, 2013 (in Japanese).

4) Haraguchi, T. and Iwamatsu, A. : Great East Japan Earthquake Tsunami detailed map, Kokin Shoin, 2011 (in Japanese).

5) Tatsuoka, F., Tateyama, M., Hirakawa, Tateyama, M., Hirakawa, D., Watanabe, K. and Kiyota, T. : Features and development history of GRS integral bridge, *Journal of Geosynthetics Engineering*, Japan chapter of IGS, Vol. 24, pp. 205-210, 2009 (in Japanese).

6) Tatsuoka, F., Kuroda, T., Yamaguchi, S., Kawabe, S. and Watanabe, K. : GRS consideration by the shaking table test of the earthquake resistance of the integrated bridge and NRB integrated bridge, *Geosynthetics Reports*, Vol. 27, pp. 141-148 , 2012 (in Japanese).

7) Railway Technical Research Institute : Design Standards for Railway Structures and Commentary (Earth retaining structure), Maruzen, 2012 (in Japanese).

8) Tamura, Y., Suyama, Y., Aoki, H., Nishioka, H. and Kato, H. : GRS positive and negative alternating horizontal loading test of reinforced embankment wall assuming a long span of integral bridges (Part 1), *48th Japan National Conference on Geotechnical Engineering*, pp. 1541-1542, 2013 (in Japanese).

9) Kato, H., Morino, T., Suyama, Y., Aoki, H., Nishioka, H. and Kojima, K. : GRS positive and negative alternating horizontal loading test of reinforced embankment wall assuming a long span of integral bridges (Part 2), *48th Japan National Conference on Geotechnical Engineering*, pp. 1543-1544, 2013 (in Japanese).

10) Kosa, K. : Study on the damage prediction and its mitigation of road structures against tsunami, Technology research and development achievements report contributing to the improvement of the quality of the road policy, No. 19-2, New Road Technology Conference, 2010 (in Japanese).

11) Shindo, Y., Yamazaki, T., Yonezawa, T., Inoue, S. and Aoki, H. : A study for the anti-tsunami of reinforced embankment integral bridges, *Japan Society of Civil Engineers 70th Annual Scientific Lecture Abstract Collection*, pp. 733-734, 2015 (in Japanese).

12) Kawabe, S., Kikuchi, Y., Watanabe, K. and Tatsuoka, F. : Model tests on the stability of GRS integral bridge against tsunami load, *Proceedings of 15th Asian Regional Conference on Soil Mechanics and Geotechnical Engineering, Fukuoka*, 2015.

13) Shindo, Y., Tamai, S., Yonezawa, T., Fujiwara, Y., Abe, M. and Shiranita, K. : Design and build of integral bridge with geosynthetic-reinforced soil and steel-reinforced concrete through girder-type superstructure, *11th Symposium Proceedings on the Use of the Composite Structure*, pp. 51-54, 2015 (in Japanese).

14) Hosaka, T., Yoda, T., Iwasaki, H. and Okada, S. : Static alternating cyclic loading experiments simulating seismic loading of a set of upper and lower integral structure connected using an anchor beam, *Japan Society of Civil Engineers Structural Engineering Reports*, Vol. 47A, pp. 1391-1401, 2001 (in Japanese).

15) Railway Technical Research Institute : Design Standards for Railway Structures and Commentary (Earth structures), Maruzen, 2007 (in Japanese).

16) Railway Technical Research Institute : Design Standards for Railway Structures and Commentary (seismic design), Maruzen, 1999 (in Japanese).

17) Sasaki, T. and Konno, T. : Restoration of soil structure of the South Riasu Line of Sanriku railway, *Engineering and Equipment*, Vol. 43, pp. 37-40, 2015 (in Japanese).